

## Parameterization of Radial Profile of Electron Cyclotron Radiation

### Power Loss in Fusion Reactor-Grade Tokamaks

K.V. Cherepanov, A.B. Kukushkin,

*NFI RRC "Kurchatov Institute", Moscow, 123182, Russia*

1. Introduction. Electron cyclotron radiation (ECR) was shown [1] to contribute significantly to local energy balance in the central part of the plasma column in the steady-state reference scenarios of tokamak ITER operation, for  $T_e(0) \sim 30$  keV and higher temperatures, becoming the dominant electron cooling mechanism in the center at temperatures exceeding 40 keV. These results are obtained via coupling of the ECR transport code CYTRAN [2] with the tokamak global transport code ASTRA.

Transport of the ECR in the fusion reactor-grade tokamaks (high temperature and strong toroidal magnetic field) is characterized by strong absorption of the radiation emitted in the hot center, in the relatively cold periphery of the plasma column [2]. Under these conditions, the distribution of the net ECR power loss density over magnetic surfaces,  $P_{EC}(r)$ , appears to be more sensitive to profiles of plasma parameters than total, volume-integrated ECR power loss. In particular, strong local enhancement of the ECR source, caused by superthermal electrons, practically would not change total ECR power loss in the ITER reference scenario 2 ( $T_e(0) \sim 25$  keV) [3].

The necessity to model the operation of reactor-grade tokamaks with fast routine transport codes (cf. [4]) requires parameterization of the profile  $P_{EC}(r)$ , in addition to parameterization [5] of the ECR total power loss. Here, on the basis of calculations with the code CYNEQ [3], we propose a parameterization to be used as a simple simulator during the transport calculations for ITER-like range of parameters.

The parameterization is based on the further simplification of the well-known fast-routine code CYTRAN [2(B)] with an accent on the satisfactory description of the profile  $P_{EC}(r)$  in the core and medium region of the plasma column, i.e. in the range of high enough temperatures, where fitting formulae [2(B)] for spectral dependence of angles-averaged absorption coefficients of EC waves in maxwellian plasmas are of good accuracy ( $\sim 20\%$  for  $10 < T_e < 120$  keV and  $\omega/\omega_B > 3$ ). Note that CYTRAN was proposed for describing  $P_{EC}(r)$  in plasmas of the advanced, low-radioactivity fuel-based reactors (D-He<sup>3</sup>, D-D, etc.) where ECR power loss appears to be the major channel of plasma cooling.

## 2. Simple analytic description of spectral temperature of outgoing EC radiation.

The analytic description of the intensity of outgoing radiation (formula (2) in [6]), which simplifies the respective approximation in [2(B)] via neglecting the diffusion-type contribution of the optically thick core of the plasma column, may be simplified further to give the following result for spectral temperature of EC radiation for extraordinary (X) and ordinary (O) waves (here mixing of the modes due to reflection from the wall is neglected):

$$T_{\text{ECR}}(\omega, K) = \langle T_{\text{cut}}(\omega, K) \rangle \left[ 1 + \frac{(1 - R_{\text{WK}})}{4\tau n_e(\rho_{\text{cut}}(\omega, K)) \chi_K(\omega, \langle T_{\text{cut}}(\omega, K) \rangle) (1 - (\rho_{\text{cut}}(\omega, K))^2)} \right]^{-1}, \quad (1)$$

where  $K = X, O$ ; and fitting formulas [2(B)] for the normalized absorption coefficients  $\chi$  are slightly modified to avoid the increasing errors at small temperatures:

$$\log_{10}(\omega^2 \chi_X(\omega, T_e)) = 1.45 - 7.8 (0.045 + (\omega - 2)/T_e)^{1/2}, \quad (2)$$

$$\log_{10}(\omega^2 \chi_O(\omega, T_e)) = 2.45 - 8.58 (0.18 + (\omega - 1)/T_e)^{1/2}, \quad (3)$$

$\tau = 6.04 \cdot 10^3 a/B_0$  is characteristic optical thickness ( $a$ , one-dimensional minor radius in meters,  $B_0$ , central magnetic field in Tesla),  $R_{\text{WK}}$  is wall reflection coefficient for  $K$  mode,

$$\langle T_{\text{cut}}(\omega, K) \rangle = (f T_{\text{cut}}(\omega, K) + (1-f) T_e(1)); \quad T_{\text{cut}}(\omega, K) = T_e(\rho_{\text{cut}}(\omega, K)); \quad (4)$$

where  $T_e = T_e(\rho)$ ,  $\rho = r/a$ ,  $f=0.6$ ; the boundary of optically thick core in the radiation's reduced phase space {frequency, radius} (cf. Eq. (1) in [6]) is described by the relations

$$\omega_{\text{cut}}/\omega_{B0} = 2 + D_K (1 - \rho_{\text{cut}} - \rho_{K\text{min}}), \quad (5)$$

$$D_K = (T_e(0) + T_e(1))/2 \{ \ln(\tau n_e(0))/C_K \}^2 + A_K, \quad A_X = 0, \quad A_O = -1, \quad (6)$$

where  $\rho_{K\text{min}} = 0.01$ ;  $C_X = 17.9$ ;  $C_O = 19.7$ ; and  $n_e(0)$  is in  $10^{20} \text{ m}^{-3}$  units. Also,  $\omega_{\text{cut}}/\omega_{B0} = 2$  for  $\rho > 1 - \rho_{K\text{min}}$ , and  $\rho_{\text{cut}} = 0$  for  $\omega/\omega_{B0} > 2 + D_K (1 - \rho_{K\text{min}})$ .

The radiation temperature  $T_{\text{ECR}}(\omega, K)$  and the respective spectral intensity are shown in Figures 1,2 for the following profiles of plasma density and temperature, taken close to those in the ITER scenarios 2 and 4 (inductive and steady-state operation, respectively), predicted by the ASTRA code 1D simulations [4] (major/minor radius 6.2/2 m,  $B_T=5.3$  T):

$$n_e(\rho) = n_e(1) + (n_e(0) - n_e(1)) [1 - \rho^2]^{0.1}, \quad n_e(0) = 10^{20} \text{ m}^{-3}, \quad n_e(1) = 0.5 * 10^{20} \text{ m}^{-3}, \quad (7)$$

$$T_e(\rho) = T_e(1) + (T_e(0) - T_e(1)) [1 - \rho^2]^{1.5}, \quad T_e(0)(\text{keV}) = 25; 24; \quad T_e(1)(\text{keV}) = 2; 0.3; \quad (8)$$

Also, the case of a higher central temperature (namely,  $T_e(0)/T_e(1) = 35/2 \text{ keV}$ ) with the same density profile is considered (Figures 3,6), as suggested by the calculations [1] for ITER steady-state operation.

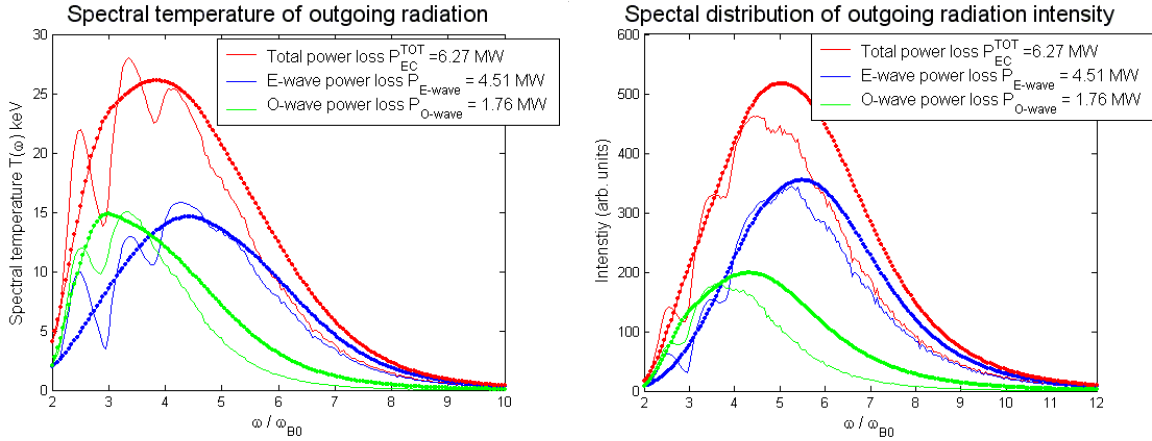


Figure 1. Spectral distribution of EC radiation temperature (left,  $T_{ECR}(\omega)$ ) and of intensity (right,  $\omega^2 T_{ECR}(\omega)$ ) of outgoing radiation for the profiles of Eqs. 7,8 with  $T_e(0) = 25$  keV,  $T_e(1) = 2$  keV, and  $R_{WK}=0.6$ . Solid – CYNEQ calculations, dots – Eq. (1). Blue, green and red curves correspond to, respectively, X and O modes, and the sum of modes.

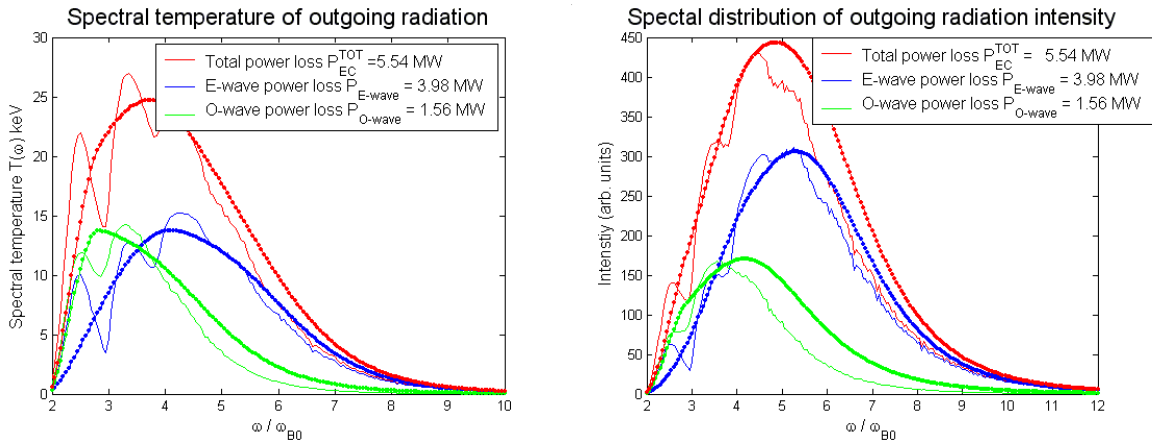


Figure 2. Similar picture for the profiles of Eqs. 7,8 with  $T_e(0) = 24$  keV,  $T_e(1) = 0.3$  keV.

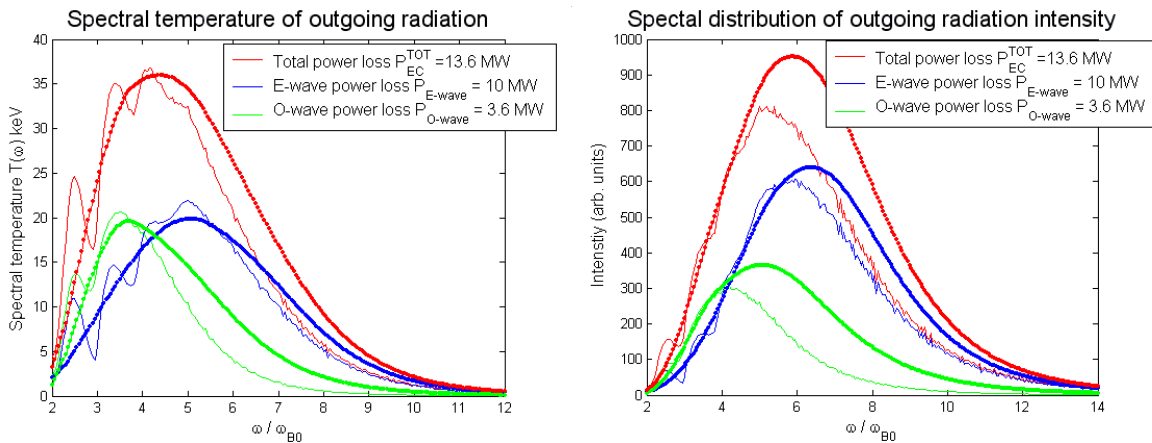


Figure 3. Similar picture for the profiles of Eqs. 7,8 with  $T_e(0) = 35$  keV,  $T_e(1) = 2$  keV.

**3. Analytic description of power loss radial profile.** Deviation of spectral temperature of EC radiation from local electron temperature determines the spectral density of the local ECR power loss in maxwellian plasmas. The remaining integration over frequency to evaluate the profile of the net radiated power,  $P_{EC}(r)$ , has to be done numerically:

$$P_{EC}(\rho) = 4\pi C \tau n_e(\rho) B_0^3 a^{-1} \sum_K \int_{\omega_{cut}(\rho)}^{\infty} \chi_K(\omega, T_e(\rho)) \tilde{\omega}^2 [T_e(\rho) - T_{ECR}(\omega, K)] d\tilde{\omega} \quad (9)$$

where  $\tilde{\omega} = \omega / \omega_{B_0}$ , and  $C = 3.9 \cdot 10^{-8} \text{ MW/m}^3$  ( $B_0$  and 'a' are in Tesla and meters).

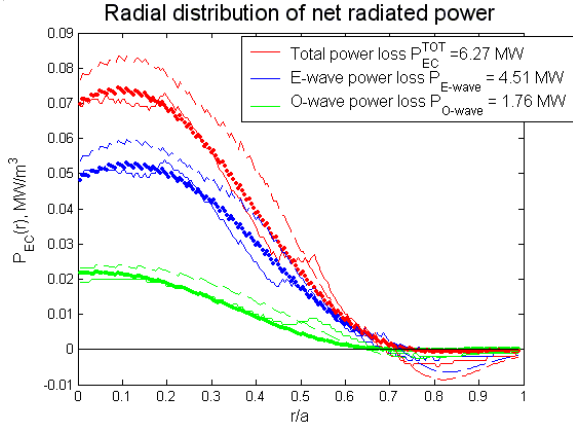


Fig. 4.

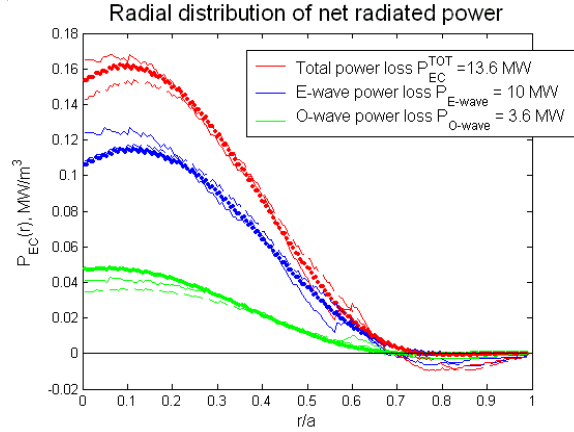


Fig. 6.

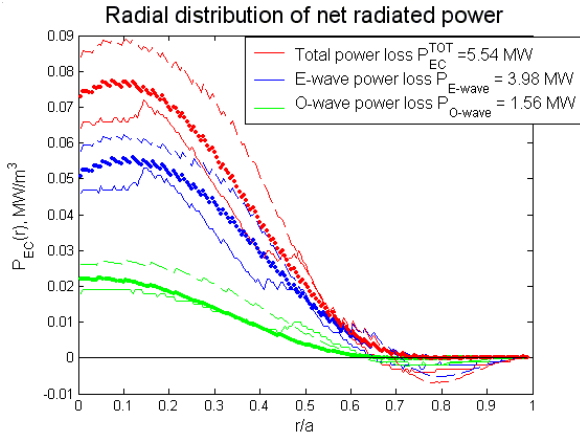


Fig. 5

The comparison of the profiles  $P_{EC}(r)$  of Eq. (9) (dots) with CYNEQ calculations (solid) and calculations of Eq. (9), where CYNEQ's numerical results for absorption coefficients  $\chi$  are used, (dashed) is given in Figures 4-6 for conditions of Figures 1-3, respectively.

**4. Conclusion.** Analysis of comparing the CYNEQ and CYTRAN calculations enabled us to simplify further the fast routine of CYTRAN and retain reasonable accuracy of describing the radial profile of

EC net radiated power,  $P_{EC}(r)$ , in the region of significant contribution of  $P_{EC}(r)$  to the local power balance in fusion reactor-grade tokamaks (first of all, in the central part of the plasma column).

**Acknowledgments.** The work is partly supported by the Russian Federal Agency on Science and Innovations (contract 02.445.11.7505) and the RF grant NSH-9878.2006.2 for Leading Research Schools.

#### REFERENCES

- [1] Albajar F., Bornatici M., Cortes G., *et al.*, Nucl. Fusion, 45 (2005) 642; Proc. 31st EPS Conf. Plasma Phys. Contr. Fusion. (London, U.K., 2004), ECA vol. 28G, P-4.171.
- [2] Tamor S., (A) Fusion Technol., 3 (1983) 293; Nucl. Instr. and Meth. Phys. Res., A271 (1988) 37; (B) Repts. SAI-023-81-110-LJ/ LAPS-72 and SAI-023-81-189-LJ/ LAPS-72, La Jolla, CA: Science Applications (1981).
- [3] Cherepanov K.V., Kukushkin A.B., Proc. 31st EPS Conf. Plasma Phys. Contr. Fusion. (London, U.K., 2004), ECA vol. 28G, P-1.175; Proc. 20th IAEA Fusion Energy Conf.. (Vilamoura, 2004), TH/P6-56.
- [4] Polevoi A.R., Medvedev S.Yu., Mukhovatov S.V., *et al.*, J Plasma Fusion Res. SERIES, 5 (2002) 82-87.
- [5] Albajar F., Bornatici M., Engelmann F., Nucl. Fusion, 42 (2002) 670.
- [6] Kukushkin A.B., Proc. 24th EPS Conf. Contr. Fusion Plasma Phys., Berchtesgaden, 1997, ECA vol. 21A, Part II, 849.